A vector-valued ground motion intensity measure incorporating normalized spectral area

Aris-Artemis I. Theophilou[1], Marios K. Chryssanthopoulos[2], Andreas J. Kappos[3]

Abstract A vector-valued intensity measure is presented, which incorporates a relative measure represented by the Normalized Spectral Area. The proposed intensity measure is intended to have high correlation with specific relative engineering demand parameters, which collectively can provide information regarding the damage state and collapse potential of the structure. Extensive dynamic analyses are carried out on a single-degree-of-freedom system with a modified Clough-Johnston hysteresis model, using a dataset of 40 ground motions, in order to investigate the proposed intensity measure characteristics. Response is expressed using the displacement ductility, and the normalized hysteretic energy, both of which are relative engineering demand parameters. Through regression analysis the correlation between the proposed intensity measure and the engineering demand parameters is evaluated. Its domain of applicability is investigated through parametric analysis, by varying the period and the strain-hardening stiffness. Desirable characteristics such as efficiency, sufficiency, and statistical independence are examined. The proposed intensity measure is contrasted to another one, with respect to its correlation to the engineering demand parameters. An approximate procedure for estimating the optimum Normalized Spectral Area is also presented. It is demonstrated that the proposed intensity measure can be used in intensity-based assessments, and in scenario-based assessments with some limitations.

Keywords Intensity measure; normalized spectral area; nonlinear response; probabilistic seismic demand assessment; ground motion selection.

1 Introduction

Probabilistic seismic response assessment is of interest both in the design of new structures, and in the assessment of existing structures. In the design of new structures the objective is to ensure that the safety level required by the building codes is fulfilled, while in the assessment of existing structures the objective is to evaluate the inherent safety level. The structural response, and hence the safety level, are best evaluated through dynamic time-history analysis, in which the intensity of the ground motion is defined by an appropriate seismic hazard analysis. A factor significantly affecting the accuracy of the response prediction is the '*ground motion selection and modification*' (GMSM) method through which the ground motion suites are formed. The GMSM method is in

[1] Faculty of Engineering and Physical Sciences, Civil Engineering, University of Surrey, Guildford, GU2 7XH, UK
email: aris@theophilou.com
[2] Faculty of Engineering and Physical Sciences, Civil Engineering, University of Surrey, Guildford, GU2 7XH, UK
[3] School of Mathematics, Computer Science & Engineering, Department of Civil Engineering, City University London, London, EC1V 0HB, UK

turn dependent on the measure used to express ground motion intensity, termed '*intensity measure*' (IM).

In the present article a vector-valued IM is presented, with which an efficient prediction of the structural response is sought. The vector-valued IM incorporates the Normalized Spectral Area parameter, $S_{dN}(T_1, T_2)$, originally proposed by Theophilou and Chryssanthopoulos (2011), which is evaluated by integration of the displacement response spectrum and normalization to the spectral displacement at the fundamental period. Due to the normalization, $S_{dN}(T_1, T_2)$ does not change when the ground motion is scaled. In this way, it captures the effect of the excitation spectrum characteristics (i.e. frequency content) on the response. The proposed IM was developed with the intention of being used in a GMSM method (Theophilou and Chryssanthopoulos 2011), in which records are normalized to the spectral acceleration at the fundamental period, $S_a(T_1)$, and the estimation of the full distribution of the response is sought.

The proposed IM is intended to exhibit high correlation with specific relative engineering demand parameters (EDPs). Collectively, these relative EDPs can provide information regarding the damage state and the collapse potential of the structure. The two relative EDPs investigated are the displacement ductility factor, μ_d, and the normalized hysteretic energy, NHE. The use of relative EDPs in seismic design/assessment has the convenience that structures with similar design characteristics have similar EDP values. For example, the displacement ductility is expected to have similar values in buildings designed to the same ductility class; in contrast, roof displacement, which is an absolute measure that depends on the height of each building, may vary significantly.

The IM is applied in the dynamic analysis of a single-degree-of-freedom (SDOF) system, in which the nonlinearity level is varied by varying the yield reduction factor. The hysteresis model adopted is the modified Clough-Johnston, which is capable of modelling stiffness degradation due to load reversals. Dynamic analyses are performed using a dataset of 40 real earthquake ground motion records.

Correlation coefficients between $S_{dN}(T_1, T_2)$ and each of μ_d, and NHE, are obtained through regression analysis. The effect of the system's fundamental period and the strain-hardening stiffness are investigated through a parametric analysis. Desirable IM characteristics such as efficiency, sufficiency, and scaling robustness are examined from the perspective of the IM correlation to the EDPs. Overall, the proposed IM is shown to perform satisfactorily over a relatively wide range of parameters.

Through examples it is demonstrated that the IM can be applied in intensity-based assessments of real systems, and in scenario-based theoretical parametric studies. The application in scenario-based assessments of real systems has certain limitations.

Finally, an approximate procedure for estimating a suitable $S_{dN}(T_1, T_2)$ is presented. The procedure uses an 'equivalent' SDOF system, the maximum displacement of which is equal to the displacement of the SDOF system considered. The procedure estimates the ultimate elongation period, which is then used in the calculation of a suitable $S_{dN}(T_1, T_2)$.

2 Motivation and framework

Predicting the response of a structure under a future earthquake can only be done in a probabilistic sense. Probabilistic seismic demand assessment aims to evaluate the mean annual frequency of exceeding an EDP, $\lambda(EDP)$, with respect to the mean annual frequency of exceeding an IM, $\lambda(IM)$. The concept is presented here using a scalar IM, and can easily be expanded to a vector-valued IM. $\lambda(EDP)$ is evaluated through the following integral (e.g. Cornell and Krawinkler 2000), which is based on the total probability theorem

$$\lambda(EDP) = \int P(EDP|IM)|d\lambda(IM)| \quad (1)$$

Evaluation of $\lambda(EDP)$ involves two distinct tasks: seismic hazard analysis, and structural analysis.

Seismic hazard analysis is performed to evaluate $\lambda(IM)$ for the earthquake scenario considered. In the first of the two general approaches, termed '*scenario-based assessment*', the known data are the seismological parameters of the earthquake source, such as the moment magnitude of the expected earthquake, the source-to-site distance, and the type of fault. It is then possible to evaluate the response at the site using a ground motion prediction model. In the second approach, termed '*intensity-based assessment*', the earthquake intensity at the site is given, usually expressed as peak ground acceleration or as $S_a(T_1)$. Most building codes convey the earthquake intensity data to the earthquake engineer through the Uniform Hazard Spectrum, which represents the peak response due to a large set of ground motions, at a specific probability of occurrence. The proposed IM can be used with both approaches.

The term $P(EDP|IM)$ expresses the probability of exceeding an EDP value given the IM value. It is evaluated through structural analysis using a dataset of ground motions, applied within the range of intensity levels of interest. The main objective of the present article is to propose an IM that results in a comparatively low variance of $EDP|IM$, $\sigma^2_{EDP|IM}$, which will result in a more accurate estimate of $\lambda(EDP)$.

The principle of reducing $\sigma^2_{EDP|IM}$ to improve the accuracy in estimating $\lambda(EDP)$ finds applicability in GMSM methods. By representing ground motion intensity through appropriate IMs, it is possible to obtain an optimized response prediction. An optimized response prediction requires a reduced number of ground motions to obtain the same level of prediction accuracy (compared to using a less efficient IM, or to random selection) or conversely, it exhibits an improved accuracy using the same number of ground motions. The present article presents the correlation between IMs and EDPs, on which the accuracy of certain GMSM methods depends. This concept has been investigated in other studies (Theophilou and Chryssanthopoulos 2011; Buratti et al. 2011), which concluded that a higher correlation between IM and EDP results in an increased accuracy in the response prediction.

The earliest IMs used were scalar, such as the spectral acceleration at the fundamental period, $S_a(T_1)$, or compound parameters, such as the $v_{max}t_d^{0.25}$ (Fajfar et al. 1990), where v_{max} is the peak ground velocity, and t_d is the time duration of ground motion. Recently the trend has shifted towards vector-valued IMs, which have the advantage of being comprised of multiple parameters, thus capturing different mechanisms that affect response. Such IMs are the $\langle S_a(T_1), \varepsilon\rangle$ by Baker and Cornell (2006), where ε is the number of standard deviations between the difference in the $\ln S_a(T_1)$ of the record and the mean $\ln S_a(T_1)$ obtained from a ground motion prediction model, and the $\langle S_a(T_1), R_{T1,T2}\rangle$ by Baker and Cornell (2006), where $R_{T1,T2}$ is the ratio $S_a(T_2)/S_a(T_1)$. Conte et al.

(2003) proposed the use of $\langle S_a(T_1), F_{R=r} \rangle$, where $F_{R=r}$ is the ratio of the minimum yield strength required to limit the response parameter R to r, to the minimum yield strength required for the system to remain elastic. Bojórquez et al. (2012) proposed $\langle S_a(T_1), I_D \rangle$, where I_D is the square of ground motion acceleration integrated with respect to the duration of the ground motion, normalized to the product of PGA and PGV (peak ground velocity), and $\langle S_a(T_1), N_p \rangle$, where N_p is the geometric mean of the spectral accelerations between the fundamental period and a higher period, normalized to $S_a(T_1)$. In all the aforementioned vector-valued IMs, the 'primary' parameter is $S_a(T_1)$, and the 'secondary' parameter is unitless. Along the same line, the vector-valued IM proposed in the present article is comprised of $S_a(T_1)$, and $S_{dN}(T_1, T_2)$.

The correlation between absolute IMs, such as Δ_{mean} (Hutchinson et al. 2002), and relative EDPs, such as μ_d, and NHE, has been found to be high in intensity-based assessments, in which ground motions were normalized to $S_a(T_1)$. However, in scenario-based assessments, in which the intensity of ground motions is expressed using seismological parameters, this correlation is negligible because $S_a(T_1)$ varies. In this article it is demonstrated that this insufficiency is relieved if the intensity is expressed using the relative measure $S_{dN}(T_1, T_2)$, in which case high correlation is observed regardless of the normalization to $S_a(T_1)$; this approach can be used in scenario-based parametric studies.

3 Dynamic analysis

3.1 Formulation

The proposed IM is used in the dynamic analysis of a SDOF system with a natural period of $T_1 =$ 1.0 sec, and viscous damping ratio of $\zeta = 5\%$. The strain hardening coefficient was taken as $\alpha =$ 3%; this value was used by Ruiz-Garcia and Miranda (2006) who concluded it plays an important role in the estimation of the residual displacement.

The hysteresis model used for the SDOF system is the modified Clough-Johnston (Clough and Johnston 1966; Mahin and Lin 1983), shown in Fig. 1, which is capable of modelling stiffness degradation due to load reversals. Its force-displacement relationship is characterized by the elastic stiffness, k_e, the strain-hardening stiffness, $k_s = \alpha k_e$, and the yield strength, f_y. The displacement capacity was assumed to be unlimited, as the purpose of the study is to evaluate the maximum displacement demand, u_m.

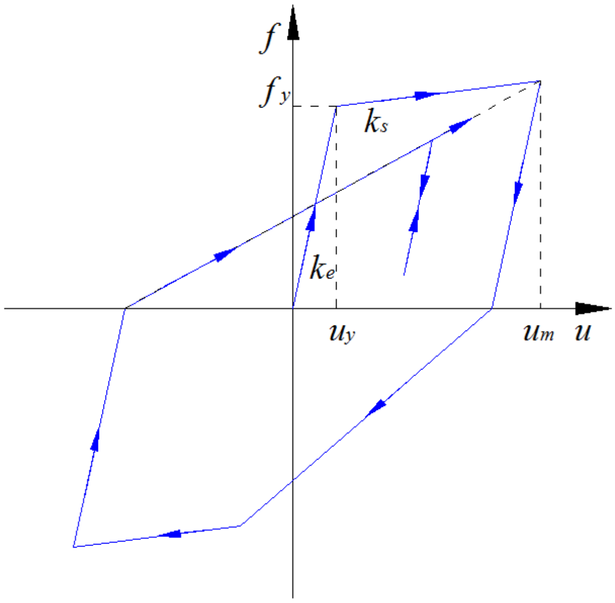

Fig. 1 Modified Clough-Johnston hysteresis model.

An equivalent elastic system having stiffness k_e was used to evaluate the maximum elastic displacement, u_0, and the maximum elastic force, f_0. The yield reduction factor, R_y, is defined as the ratio of f_0 to the yield strength, f_y, or equivalently as the ratio of u_0 to the yield displacement, u_y, as shown below

$$R_y = \frac{f_0}{f_y} = \frac{u_0}{u_y} \tag{2}$$

For every ground motion the spectral displacement, $S_d(T_1)$, is taken as equal to u_0.

The equation of motion for a SDOF system (Jacobsen 1930) is recast to account for the nonlinear force-displacement relationship, $f(u)$, shown in Fig. 1, normalized to u_y, and using R_y on the right hand side to express intensity, as shown below

$$\frac{\ddot{u}}{u_y} + 2\zeta\omega_n \frac{\dot{u}}{u_y} + \frac{f(u)}{mu_y} = -R_y \frac{\ddot{u}_g(t)}{u_0} \tag{3}$$

where $\ddot{u}$, $\dot{u}$, and u, are the acceleration, velocity, and displacement of the system respectively, ω_n is the natural circular frequency, m is the mass, and $\ddot{u}_g(t)$ is the ground acceleration.

Equation (3) shows that if $\ddot{u}_g(t)$ is scaled, while R_y is kept unchanged, the response ratio u/u_y remains unchanged. This happens because scaling $\ddot{u}_g(t)$ causes an equal scaling of u_0, so the ratio $\ddot{u}_g(t)/u_0$ remains unchanged. One way of keeping R_y unchanged is by simultaneously scaling $\ddot{u}_g(t)$ and u_y by the same factor, so that u_0/u_y remains unchanged.

4 Dataset of ground motion records

A ground motion record dataset was formed by selecting 40 records from the European Strong-Motion Database (Ambraseys et al. 2002) and the NGA Database 2005 (PEER Center 2005), summarized in Table A1, with seismological characteristics similar to those of the considered earthquake scenario. The earthquake scenario has been conditioned to be a strong earthquake, at a site with rock ground conditions, at close distance from the fault, but sufficiently distant to avoid near-fault effects.

The criteria used in the selection of the records are the following: (1) the moment magnitude is higher than 6, (2) the closest distance from fault is not larger than about 30 km, so that the attenuation of the seismic ground motion is sufficiently low, (3) records do not exhibit near-fault effects, such as velocity pulses of distinctly long period, (4) records from not more than two accelerographs from each earthquake event were used, (5) accelerographs were installed on free-field conditions, or on one- to four-storey lightweight structures located at the lowest level, (6) accelerographs were installed on rock ground conditions with $V_{S30} \geq 650\ \mathrm{m/sec}$, where V_{S30} is the shear wave velocity in the top 30 m of the ground, and (7) selection was such that the dataset includes records from a variety of worldwide locations.

4.1 Approach for estimating response distribution

The goal in performing the dynamic analyses is to evaluate the probability distribution of the response with respect to a particular intensity level, or a range of intensity levels. In this section the rationale is presented as to why intensity should be expressed in terms of R_y, which is a '*relative measure*', rather than spectral displacement, $S_d(T_1)$, which is an '*absolute measure*'.

To estimate the response distribution with good accuracy, all records should be considered. As different records exhibit different $S_d(T_1)$ values, scaling needs to take place. Ideally, scale factors applied should not be much higher than the upper limits of 3 (Shome et al. 1998) or 4 (Iervolino and Cornell 2005). For the particular dataset used herein, the $S_d(T_1)$ of the unscaled records had a maximum to minimum ratio of 56. If intensity was expressed in terms of $S_d(T_1)$, and records were normalized to the highest $S_d(T_1)$, unrealistically high scale factors would have been applied.

Thus, the issue of scaling ground motions was tackled from a different angle, by expressing intensity in terms of R_y, which represents the degree of nonlinearity experienced by the structure. In this way, at a given intensity level a uniform scale factor was applied to all ground motions. The physical meaning of increasing R_y is that ground motion is scaled up provided that u_y is equal to u_0 of the unscaled ground motion, and that u_y remains unchanged throughout scaling; it can be deduced from equation (3) that R_y is equal to the scale factor. A range of ground motion intensities was investigated, by increasing R_y from 1 to 8, based on reaching the highest values (e.g. 8.5, ICBO 1997) found in building codes.

4.2 Engineering demand parameters

The EDPs investigated are μ_d, and NHE, both of which are relative EDPs. μ_d is a function of the ratio u/u_y, and NHE is a function of the ratios u/u_y and f/f_y; it can be seen from equation (3) that both ratios depend on R_y. Since $R_y = u_0/u_y$, it is inferred that the EDPs are not necessarily dependent on u_0 (and hence $S_d(T_1)$), and u_y, when either is considered individually. In other words, if u_0 is doubled, this does not by itself infer that R_y is also doubled; information about u_y is also needed to derive such a conclusion.

The relative EDPs chosen to be investigated in the present study can be used collectively to provide an estimate of the structural damage state and collapse potential. One such application are damage indexes, such as the widely used Park-Ang index (Park and Ang 1985; Park et al. 1985), that are functions of a displacement-based EDP (e.g. maximum displacement), and an energy-based EDP (e.g. hysteretic energy dissipated).

4.2.1. Displacement ductility factor

Displacement ductility factor (DDF), μ_d, is the degree of inelastic displacement that the structure can experience before failure, defined as

$$\mu_d = \frac{u_m}{u_y} \tag{4}$$

Fig. 2(a) shows the mean μ_d of all dynamic analyses, and Fig. 2(b) shows the coefficient of variation (COV) of μ_d. The estimates are compared to the relationships proposed by Ruiz-Garcia and Miranda (2003) derived through a statistical study using 216 records on a SDOF system with bilinear hysteresis. It is observed that the overall trends are similar in each graph, with the mean curves displaying better consistency than the COV curves.

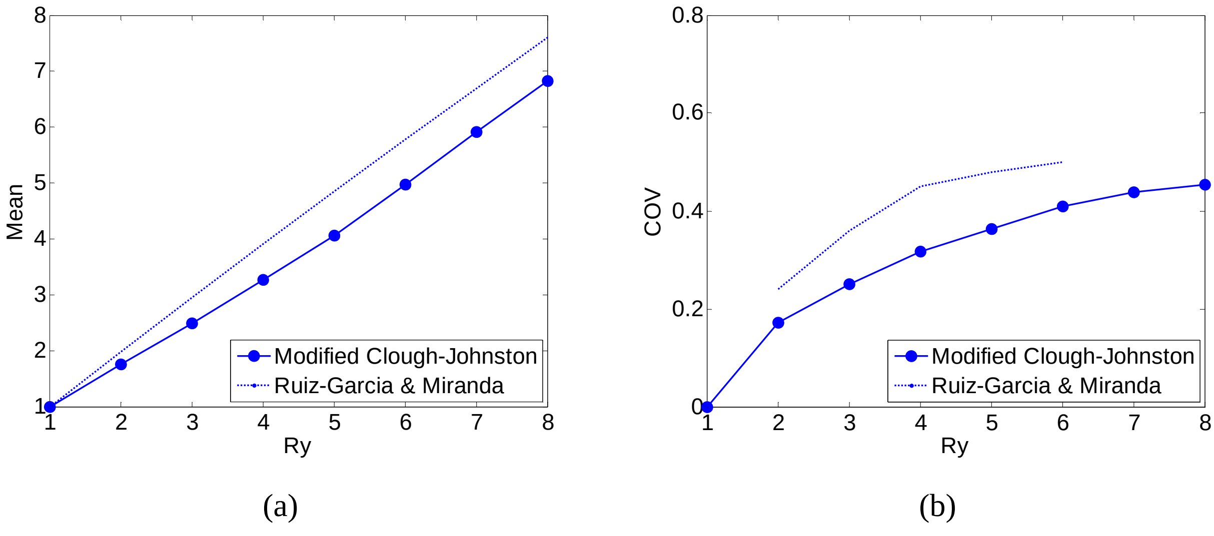

Fig. 2 (a) Mean μ_d, and (b) COV of μ_d.

4.2.2. Normalized Hysteretic Energy

Normalized Hysteretic Energy (Mahin and Bertero 1981), NHE, is defined as the cumulative amount of the hysteretic energy dissipated, E_H, normalized to the work required by the SDOF system to yield under monotonically increasing loading, given by the following equation

$$NHE = \frac{E_H}{f_y u_y} \tag{5}$$

Fig. 3(a) shows the mean NHE of all dynamic analyses, and Fig. 3(b) shows the COV.

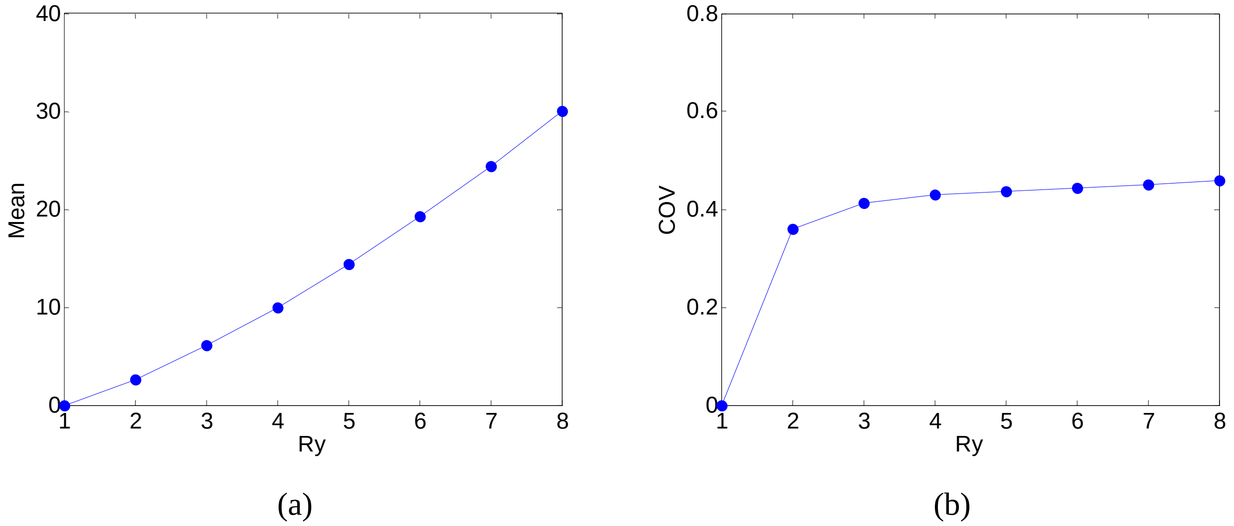

Fig. 3 (a) Mean NHE, and (b) COV of NHE.

5 Proposed intensity measure

The proposed vector-valued IM is denoted as

$$\langle S_a(T_1), S_{dN}(T_1, T_2)\rangle \tag{6}$$

The first vector element is $S_a(T_1)$, which is an absolute measure. $S_a(T_1)$ can be taken directly from most building codes and ground motion prediction models. It is required in the definition of the proposed IM to provide the level of intensity, given that the other vector element is relative and hence unitless.

The second vector element is $S_{dN}(T_1, T_2)$, which is a relative measure, given by

$$S_{dN}(T_1, T_2) = \frac{1}{S_d(T_1) T_N} \int_{T_1}^{T_2} S_d(T) dT\,, \quad T_1 < T_2 \tag{7}$$

where T_1 is the initial fundamental period of the system, T_2 is an approximation of the elongated period of the system due to inelastic effects, $T_N = 1.0$ sec is a normalizing constant.

$S_{dN}(T_1, T_2)$ is evaluated by integration of the displacement response spectrum from T_1 to T_2, and normalization to $S_d(T_1)$. The normalization constant T_N is not dependent on either T_1 or T_2. Due to normalization, the $S_{dN}(T_1, T_2)$ value does not change when ground motion is scaled. $S_{dN}(T_1, T_2)$ is statistically independent of $S_d(T_1)$, as explained later. In this way, $S_{dN}(T_1, T_2)$ captures the effect of the excitation spectral characteristics (i.e. frequency content) on the response. Thus, it is a measure of intensity that affects the inelastic response associated with period elongation. In turn, the degree of period elongation depends on the frequency content, which is unique for each ground motion. Hence, the purpose of integrating the response spectrum is to capture the elongated period within appropriately estimated bounds.

$S_{dN}(T_1, T_2)$ provides an indication of the local response spectrum shape between periods T_1 and T_2. As noted in Fig. 4, which shows three displacement response spectra normalized to $S_d(T_1)$, the value of this parameter is subject to considerable variation.

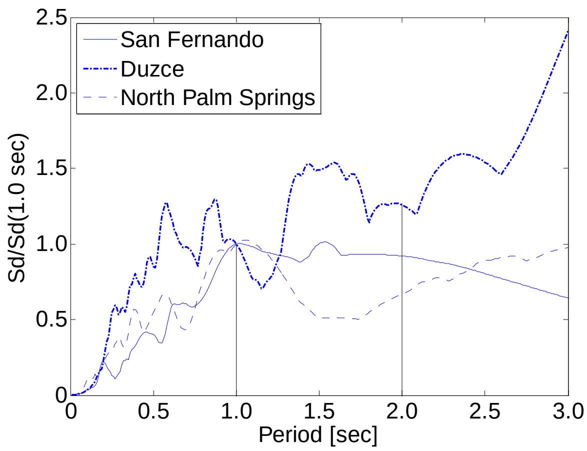

Fig. 4 Normalized Spectral Area between periods $T_1 = 1.0$ sec, $T_2 = 2.0$ sec : North Palm Springs $S_{dN}(1.0{,}2.0) = 0.69$, San Fernando $S_{dN}(1.0{,}2.0) = 0.95$, Duzce $S_{dN}(1.0{,}2.0) = 1.24$.

6 Statistical dependence between intensity and response

6.1 Regression analysis

Regression analyses were carried out between the IM and the EDPs, to find suitable models that describe their relationship and to evaluate their correlation. Regression analyses were carried out at each R_y level, by considering as the two regression variables $S_{dN}(T_1, T_2)$, and each of the EDPs.

The probability distribution of $S_{dN}(T_1, T_2)$ was evaluated for the integration intervals from $T_1 = 1.0$ sec to $T_2 = 1.4, 1.6, 1.8, 2.0$, and 2.2 sec. The empirical distribution of $S_{dN}(T_1, T_2)$ was then tested for conformity to the normal and lognormal distributions. The first method employed was Lilliefors test (Lilliefors 1967; Van Soest 1967), and the second method was visual inspection of the cumulative distribution graphs, shown in Fig. 5. It was concluded that the empirical distribution of $S_{dN}(T_1, T_2)$ can be characterized well by both distributions, at a significance level of $\alpha_s = 5\%$.

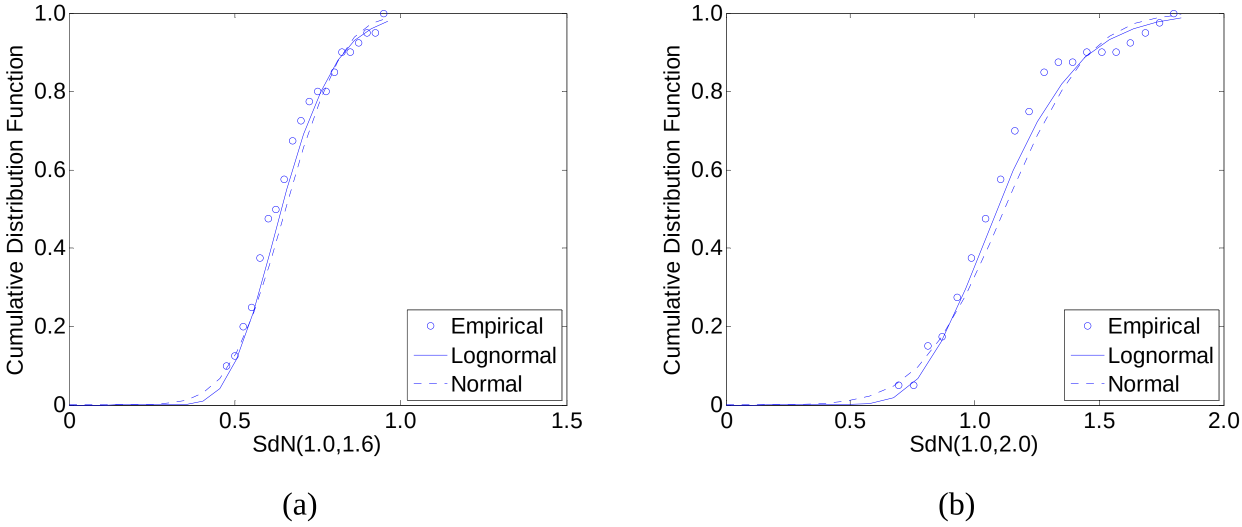

Fig. 5 Cumulative distribution function of (a) $S_{dN}(1.0,1.6)$, and (b) $S_{dN}(1.0,2.0)$.

The empirical probability distribution of the EDPs was evaluated at each R_y level. For each EDP Lilliefors test was used to determine the conformity of the empirical distribution to a known distribution, at a significance level of $\alpha_s = 5\%$. Lilliefors test was complemented by a visual inspection of the cumulative distribution graphs. As a result, the distributions of both μ_d, and NHE, were found to be lognormal.

For the relationship between $\ln\left(S_{dN}(T_1,T_2)\right)$ and each of $\ln(\mu_d)$, and $\ln(NHE)$ the simple linear regression model was adopted at each R_y level. An important conclusion is that the simple linear regression model is suitable for describing these relationships. This is illustrated in Fig. 6, which shows that the regression lines describe well the raw data.

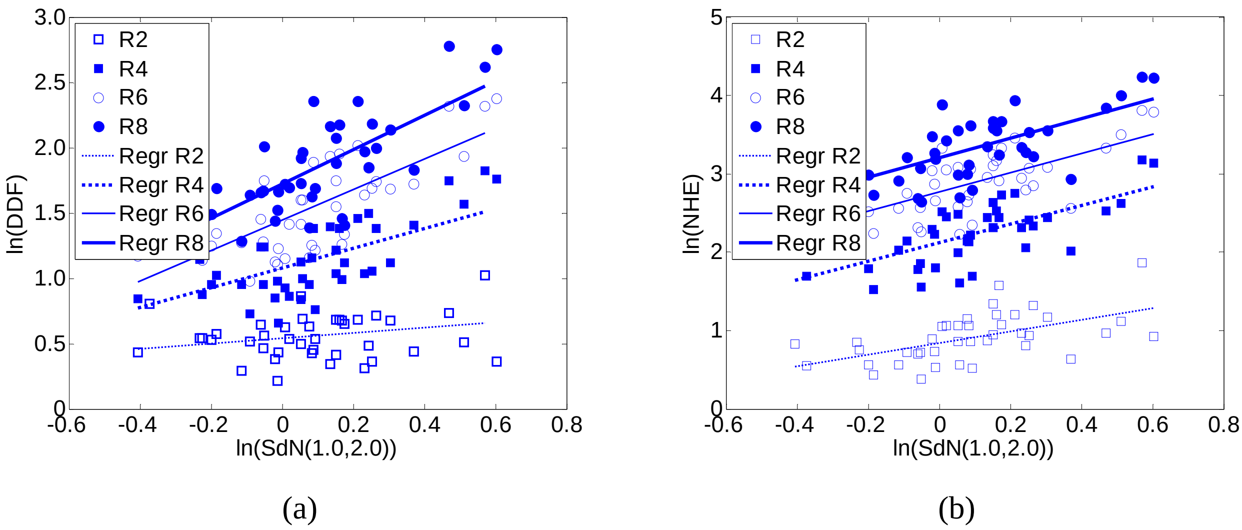

Fig. 6 Regression analysis between $\ln\left(S_{dN}(1.0,2.0)\right)$ and (a) $\ln(\mu_d)$, (b) $\ln(NHE)$.

The correlation coefficient, ρ, between $\ln\left(S_{dN}(T_1,T_2)\right)$ and each of $\ln(\mu_d)$, and $\ln(NHE)$ was estimated through the Pearson sample correlation coefficient, shown in Fig. 7.

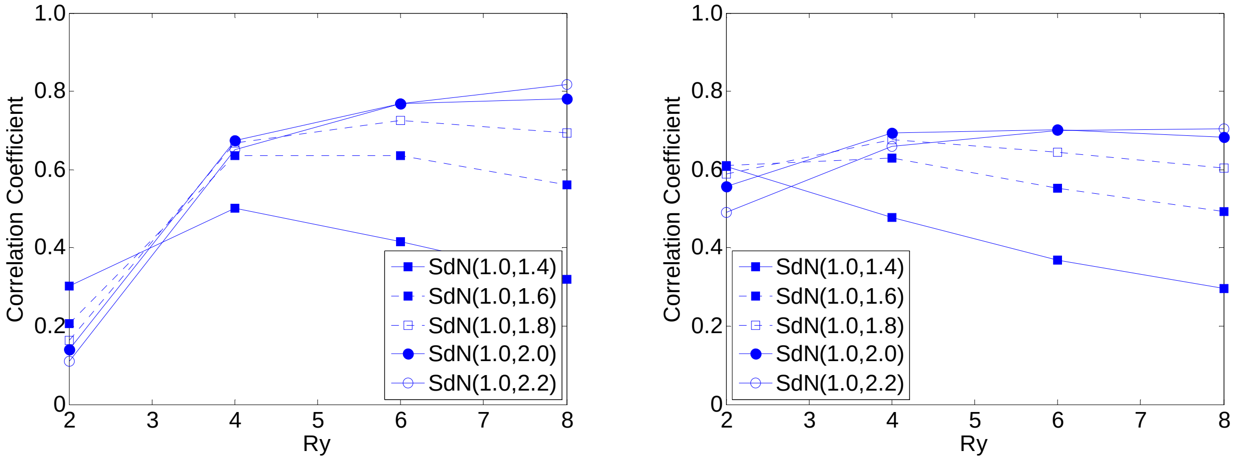

(a) (b)

Fig. 7 Correlation coefficients, ρ, between $\ln\left(S_{dN}(T_1, T_2)\right)$ and (a) $\ln(\mu_d)$, (b) $\ln(NHE)$.

It can be observed that ρ is generally high, in the range 0.6-0.8, for both relationships. It is also observed that ρ varies with R_y (i.e. the nonlinearity level). Some discrepancies exist between the ρ curves in each graph. These are attributed to the T_2 value used, which is assumed to match the elongated period of the structure. At very low nonlinearity levels, i.e. $R_y = 2$, the highest ρ is obtained using $T_2 = 1.4$ sec, while at moderate to high nonlinearity levels, i.e. $R_y = 4 - 8$, using $T_2 = 1.6 - 2.2$ sec results in the highest ρ. Misestimating the true elongated period results in a ρ lower than the highest possible ρ. It is therefore confirmed that the T_2 value at which the highest ρ is observed is dependent on the nonlinearity level.

6.2 Parametric analysis

The previous regression analyses were conducted for a SDOF system with specific parameters. To generalize these conclusions and investigate the domain of applicability of the IM, a parametric analysis was carried out. The two variables considered were T_1, between 0.5 sec and 2.5 sec, and α, between 3%-10% (Ruiz-Garcia and Miranda 2006). For the purposes of the parametric analysis T_2 was taken as equal to $2.0T_1$ throughout, which is an upper bound approximation of the elongated period at the high nonlinearity levels, as suggested in some previous studies (Bojórquez and Iervolino 2011, Cordova et al. 2001).

Using Lilliefors test the probability distribution of $S_{dN}(1.5{,}3.0)$ was found to conform well to the normal and lognormal distributions, and the distributions of $S_{dN}(0.5{,}1.0)$ and $S_{dN}(2.0{,}4.0)$ were found to conform well to the lognormal distribution, at a significance level of $\alpha_s = 5\%$. The distribution of $S_{dN}(2.5{,}5.0)$ was found not to conform to either the normal or the lognormal distributions, hence $T_1 = 2.5$ sec was rejected as exceeding the domain of applicability.

Regression analysis was carried out using the simple linear model, for each (T_1, α) combination, to find ρ between $\ln\left(S_{dN}(T_1, T_2)\right)$, and each of $\ln(\mu_d)$, and $\ln(NHE)$. Fig. 8, and Fig. 9 show ρ

plotted against R_y, at $\alpha = 3\%$, and $\alpha = 10\%$, respectively. It can be observed that the ρ trends are similar between the two figures, and also similar to the trends in Fig. 7. In particular, the maximum ρ reached is in the range 0.6-0.9 for both $\ln(\mu_d)$, and $\ln(NHE)$. From the high ρ observed it is concluded that $S_{dN}(T_1, T_2)$ is applicable within the domain of $T_1 = 0.5 - 2.0$ sec, and $\alpha = 3\% - 10\%$.

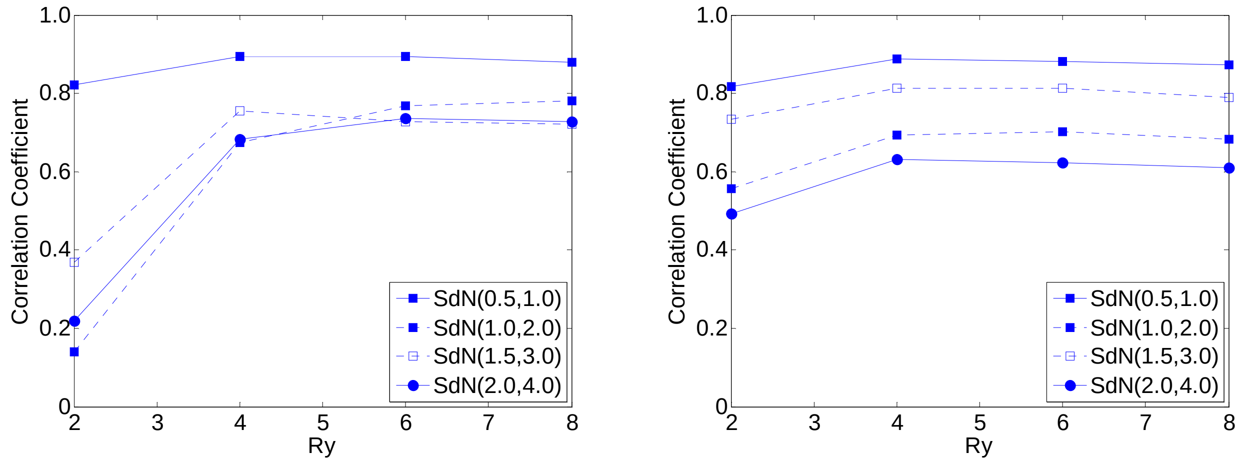

(a) (b)

Fig. 8 Correlation coefficients between $\ln\left(S_{dN}(T_1, T_2)\right)$ and (a) $\ln(\mu_d)$, (b) $\ln(NHE)$, at $\alpha = 3\%$.

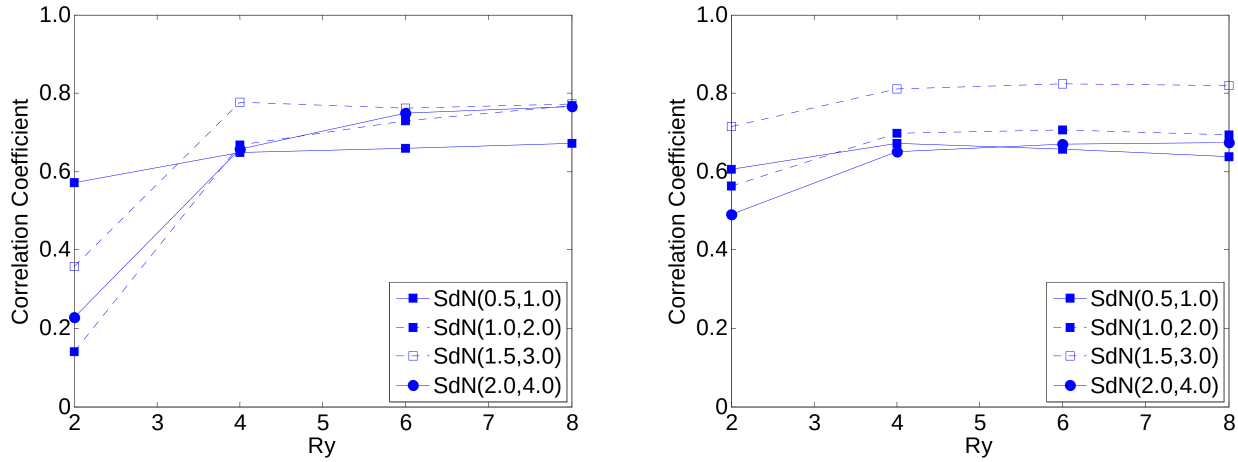

(a) (b)

Fig. 9 Correlation coefficients between $\ln\left(S_{dN}(T_1, T_2)\right)$ and (a) $\ln(\mu_d)$, (b) $\ln(NHE)$, at $\alpha = 10\%$.

6.3 Estimation error in the correlation coefficient

The estimation error in ρ can be calculated using '*Fisher-z*' transformation (e.g. Sachs 1984). In Fisher-z transformation the standard error is given by $(N - 3)^{-1/2}$, where N is the sample size. In the present regression analysis the sample size is 40, which corresponds to a standard error of 16%. This order of standard error is deemed higher than the desirable, which would ideally be 5-10%, yet it is a result of the limitation in available records.

6.4 Correlation of $S_{dN}(T_1, T_2)$ to other variables

Regression analysis was carried out between $S_{dN}(T_1, T_2)$ ($T_2 = 2.0T_1$), as the first regression variable, and each of $S_d(T_1)$, moment magnitude (M), and Significant Duration (SD) (Trifunac and Brady 1975), as the second regression variable, within the T_1 range 0.5-2.0 sec. Fig. 10 shows the correlation coefficient, ρ, plotted against T_1. Such low correlation levels infer that these parameters can be assumed to be statistically independent, and therefore the IM can be used throughout the entire T_1 range investigated. Another analysis was carried out between the natural logarithms of these variables, with similar results.

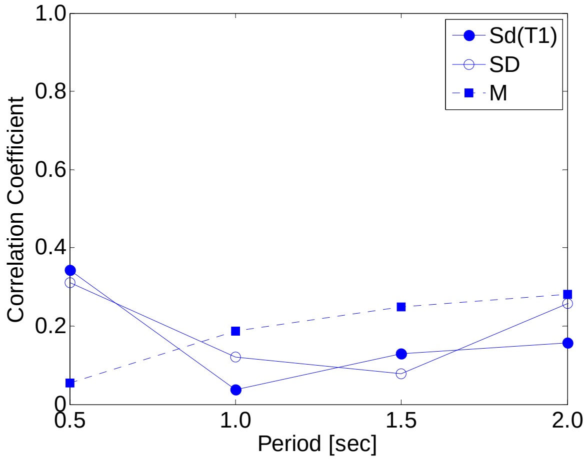

Fig. 10 Correlation coefficient between $S_{dN}(T_1, T_2)$ and (a) $S_d(T_1)$, (b) moment magnitude, and (c) Significant Duration.

7 Appraisal of proposed intensity measure

7.1 Desirable intensity measure characteristics

Desirable characteristics of IMs are efficiency, sufficiency, and scaling robustness.

Efficiency is the relatively low variance of the predicted EDP given the IM, $\sigma^2_{EDP|IM}$, obtained using

$$\sigma^2_{EDP|IM} = (1 - \rho^2)\sigma^2_{EDP} \tag{8}$$

where σ^2_{EDP} is the variance of the EDP.

Equation (8) shows that the higher the ρ, the lower is the $\sigma^2_{EDP|IM}$. The high ρ found, in the range 0.6-0.8, infer that $\sigma^2_{EDP|IM}$ is relatively low, especially at $R_y \geq 4$. Furthermore, the efficiency should be seen with respect to the objective for which the proposed IM was developed, which, as mentioned earlier, is to be used in a GMSM method. Theophilou (2013) found that significant reduction in computational work results when using the proposed IM with a GMSM method for the response prediction of a SDOF system, due to the reduced number of records required to achieve the same prediction accuracy. Therefore the proposed IM can be characterized as efficient.

Sufficiency is the degree by which an IM can be used independently of any other seismological parameter, in estimating the probability $P(EDP|IM)$. Sufficiency can be expressed in terms of $|\rho|$: the higher the $|\rho|$, the lower the dependency of the EDPs on other parameters. At the upper limit, $|\rho| = 1.0$, the EDP is a deterministic function of the IM, hence the former depends entirely on the latter; at the lower limit, $\rho = 0$, the EDP is independent of the IM. The high ρ found, in the range 0.6-0.8, infer that the presented IM is highly sufficient, given the substantial variance of the seismological parameters of the ground motions, some of which are presented in Table A1. The high sufficiency is further evidenced by the low correlation to SD, M, and $S_d(T_1)$, as shown previously in Fig. 10.

Scaling robustness is the degree by which using an IM results in an unbiased EDP estimation after scaling. As described earlier in this article, the EDPs examined are dependent on R_y. Between $R_y = 4$ and $R_y = 8$, which correspond to scale factors of 4 and 8, respectively (by scaling up $\ddot{u}_g$ and keeping u_y constant), it is observed that there is no significant change in ρ, which is maintained at high levels, in the range 0.6-0.8, for both μ_d, and NHE. The high correlation at the moderate to high nonlinearity levels infers that the concept on which the development of $S_{dN}(T_1, T_2)$ is based (i.e. that it tracks the elongated period on the response spectrum) stands true. If it is assumed that scale factors of 4 are legitimate, as Iervolino and Cornell (2005) suggest, then this is an indication that scale factors of 8 are also legitimate. This argument is based on the assumption that ground motion characteristics can be extrapolated to the intensity of the scaled record. It is possible, however, that other epistemic uncertainties invalidate this assumption, such as the frequency content of higher intensity earthquakes. Further cross-bin scaling comparisons are needed, which in practice cannot always be achieved due to the scarcity of high intensity records, if more reliable conclusions are to be derived with regard to the distortion caused by scaling.

7.2 Comparison to epsilon

The proposed IM was compared to $\langle S_a(T_1), \varepsilon \rangle$ (Baker and Cornell 2006). Similarly to $S_{dN}(T_1, T_2)$, epsilon, ε, is an indicator of the response spectrum shape. The equation for epsilon, ε, is given below

$$\varepsilon = \frac{\ln S_a(T_1) - \mu_{\ln S_a}(M, R, T_1)}{\sigma_{\ln S_a}(M, R, T_1)} \tag{9}$$

where R is the distance to the fault.

The compared parameter was the correlation coefficient, ρ, between the IMs and each of the EDPs considered in this study, evaluated in the R_y range from 2 to 8. The random variable of vector $\langle S_a(T_1), \varepsilon \rangle$ considered was epsilon, ε, which is independent of scaling, and hence is also independent of $S_a(T_1)$.

The probability distribution of ε was found to be normal, using Lilliefors test and by visual inspection of the cumulative distribution graphs. The simple linear model was adopted in the regression analysis. To investigate the effect of T_1, a parametric analysis was also conducted by varying T_1 between 0.5 and 2.0 sec. The $|\rho|$ (shown as absolute value because ρ is negative for ε) of each EDP are shown in Fig. 11.

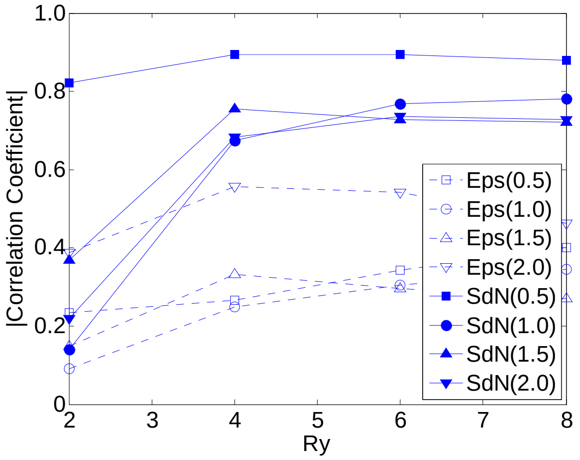

(a)

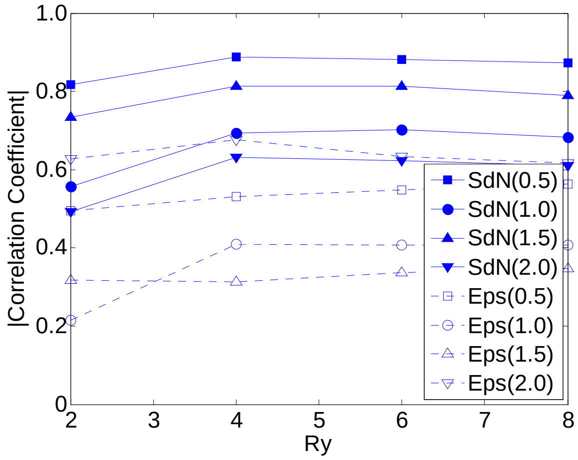

(b)

Fig. 11 Correlation coefficients between various IMs and (a) $\ln(\mu_d)$, (b) $\ln(NHE)$ (Eps(T): Epsilon at T, $S_{dN}(T_1)$: $S_{dN}(T_1, 2.0T_1)$).

It is observed in Fig. 11 that $S_{dN}(T_1, T_2)$ has a generally much higher $|\rho|$ than ε.

The high efficiency of ε in estimating the inelastic response of a SDOF system is attributed to the fact that it contains information about the tendency of the response spectrum shape in the elongated period region (Baker and Cornell 2006). For two ground motions scaled to the same $S_a(T_1)$, the ground motion with lower ε tends to have a higher inelastic displacement, since the response in the elongated period region tends to be higher. However, ε is influenced by other characteristics of the response spectrum which are not related to the inelastic response of the SDOF system, such as the period region below T_1 and the period region beyond T_2. $S_{dN}(T_1, T_2)$ is potentially more efficient than ε in estimating the inelastic response, because it is bounded between T_1 and T_2, thus excluding the period ranges that do not affect the response.

7.3 Using IM with GMSM methods

The implication of high ρ is that using the proposed IM with certain GMSM methods (Theophilou 2013) is expected to result in an optimized response prediction, compared to using an IM with lower ρ, or to random selection. Different T_2 should be used with respect to the nonlinearity level, so as to obtain the peak ρ, on which the accuracy of the prediction depends. This observation can affect ground motion selection, as applied in building codes.

7.4 Correlation between intensity and response using absolute and relative measures

In this section it is explained that there is a conceptual difference between the correlation of a relative IM, such as $S_{dN}(T_1, T_2)$, with a relative EDP, such as μ_d, and the correlation of an absolute IM, such as the Mean Spectral Displacement, Δ_{mean} (Hutchinson et al. 2002), defined in (10), with a relative EDP, such as μ_d.

$$\Delta_{mean} = \frac{1}{T_2 - T_1} \int_{T_1}^{T_2} S_d(T) dT \,, \quad T_1 < T_2 \tag{10}$$

In the first example, a SDOF system with a given u_y is considered. As the EDPs examined are independent of u_y (when considered individually), the latter can correspond to any value. All ground motions are normalized with respect to u_0 (i.e. $S_d(T_1)$) at any given R_y, which is consistent with the intensity-based approach. The correlation between $\ln\left(S_{dN}(T_1, T_2)\right)$ and $\ln(\mu_d)$, and between $\ln(\Delta_{mean})$ and $\ln(\mu_d)$ are plotted in Fig. 12(a), using $T_1 = 1.0$ sec, and $T_2 = 2.0$ sec. It can be observed that the difference between the two lines is very small, which is attributed to the fact that the coefficient of variation of $\ln\left(S_{dN}(T_1, T_2)\right)$ is approximately equal to the coefficient of variation of $\ln(\Delta_{mean})$. Similar trend is observed in the correlation between $\ln\left(S_{dN}(T_1, T_2)\right)$ and $\ln(NHE)$, and between $\ln(\Delta_{mean})$ and $\ln(NHE)$, plotted in Fig. 12(b).

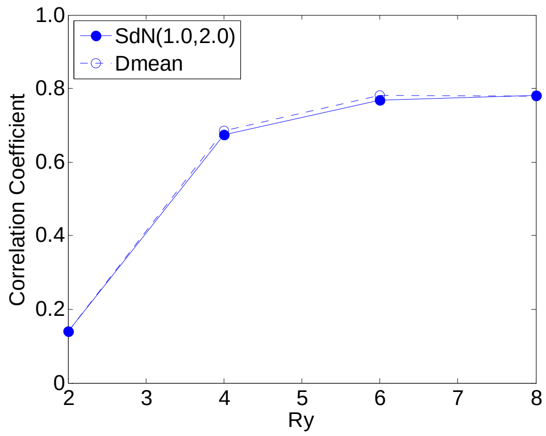

(a)

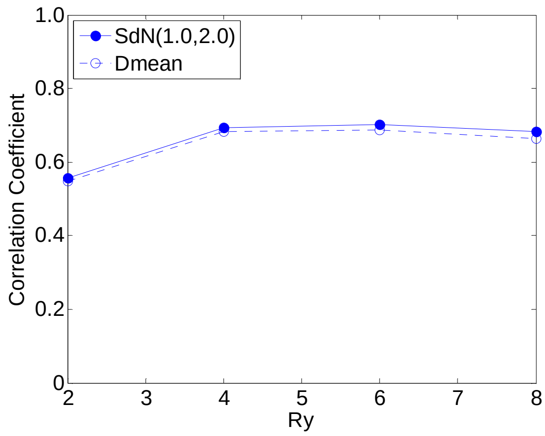

(b)

Fig. 12 Correlation coefficient between the IMs and (a) μ_d, (b) NHE, for a system with given u_y.

In the second example, the ground motions match a particular earthquake scenario, defined by seismological parameters such as the magnitude and distance from fault. This is consistent with "objectives 1 and 2" in PEER Report 2009/01 (Haselton 2009), which allow for ground motions to be selected in this way. The system u_y is taken as equal to u_0, for each unscaled ground motion, in this way applying a uniform scale factor to all ground motions. This is a theoretical example that can be used in parametric studies, whereas the previous example corresponds to a real system. The correlation between $\ln\left(S_{dN}(T_1, T_2)\right)$ and $\ln(\mu_d)$, and between $\ln(\Delta_{mean})$ and $\ln(\mu_d)$, are plotted in Fig. 13, using $T_1 = 1.0$ sec, and $T_2 = 2.0$ sec. It can be observed that the correlation between $\ln\left(S_{dN}(T_1, T_2)\right)$ and $\ln(\mu_d)$ is the same as in the previous example, which is attributed to the fact that the two measures are relative and hence unitless, thus, they do not change with scaling. In contrast, the correlation between $\ln(\Delta_{mean})$ and $\ln(\mu_d)$ is so low that can be regarded as zero, which is attributed to the fact that Δ_{mean} is an absolute measure, whereas μ_d is a relative measure. Similar trend is observed in the correlation between $\ln(S_{dN}(T_1, T_2))$ and $\ln(NHE)$, and between $\ln(\Delta_{mean})$ and $\ln(NHE)$, plotted in Fig. 13(b).

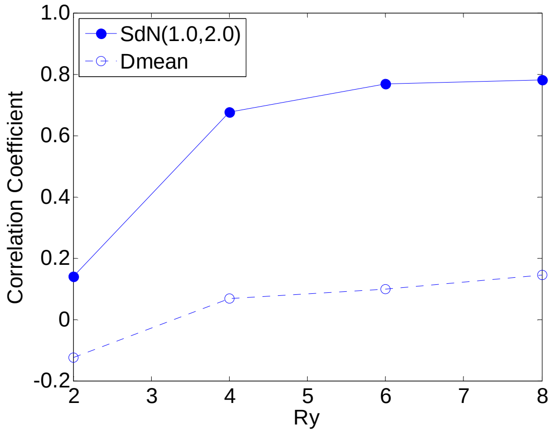

(a)

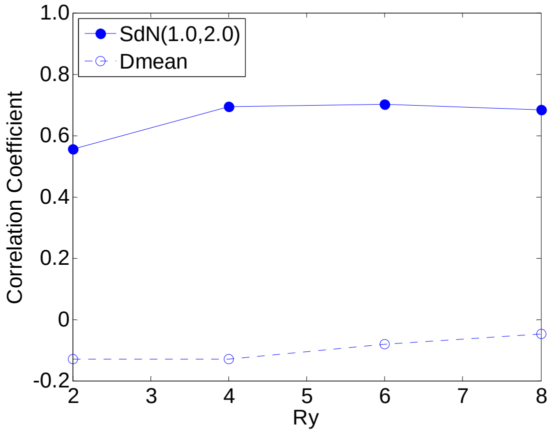

(b)

Fig. 13 Correlation coefficient between the IMs and (a) μ_d, (b) NHE, for systems with u_y not normalized.

It is, therefore, concluded that the correlation between a relative IM, such as $S_{dN}(T_1, T_2)$, and a relative EDP, such as μ_d, and NHE, is not dependent on the normalization of the ground motions. In contrast, the correlation between an absolute IM, such as Δ_{mean}, and a relative EDP, such as μ_d, and NHE, is dependent on the normalization of the ground motions. The same concept applies with other absolute IMs based on spectrum integration, such as the classical Spectral Intensity (Housner 1952), the Acceleration Spectrum Intensity (Von Thun et al. 1988), the Displacement Spectrum Intensity (Bradley 2011). This infers that the proposed IM can be used in both intensity-based assessments, where ground motions are normalized, and also in scenario-based parametric studies, where ground motions are not normalized.

7.5 Limitation of proposed intensity measure

The proposed IM presents a limitation when applied in scenario-based assessments. This is exemplified using a SDOF system with $T_1 = 1.0$ sec and $u_y = 0.010$ m. The ground motions are scaled to match a particular earthquake scenario, defined by a moment magnitude of 8.5 and distance from fault of 15 km, adopting the procedure proposed by Ay and Akkar (2012). With this procedure a different scale factor is applied to each ground motion. The advantage of selecting ground motions in this way is that the aleatory variance in $S_a(T_1)$ is maintained. The entire dataset of 40 ground motions has a coefficient of variation in $S_a(T_1)$ of 0.83, and negligible correlation between $\ln(S_{dN}(T_1, T_2))$ and $\ln(\mu_d)$. It appears that this is a limitation of the proposed IM, attributed to the relatively high variance in $S_a(T_1)$, which results in a relatively high variance in the nonlinearity level. This limitation can be alleviated by selecting a subset of 10 ground motions, by eliminating the 15 lowest and the 15 highest $S_a(T_1)$. This subset has a reduced coefficient of variation in $S_a(T_1)$ of 0.13, and a correlation between $\ln\left(S_{dN}(1.0,1.8)\right)$ and $\ln(\mu_d)$ of 0.66. This correlation level is similar to the one obtained using a uniform scale factor throughout.

8 Practical application

8.1 Estimation of T_2

To obtain the most accurate response prediction, the optimum value of $S_{dN}(T_1, T_2)$ should be used. At the optimum $S_{dN}(T_1, T_2)$ the highest correlation to the EDPs is observed. This requires the estimation of the corresponding T_2, which represents the highest elongated period of the SDOF system and is a function of the nonlinearity level. Theoretically, the user should first perform a rigorous regression analysis, with which to obtain correlation graphs similar those in Fig. 7, and subsequently select the optimum T_2. In practice, however, this is a very computationally expensive task, and furthermore this task may be impeded by the limited number of available records. In this section a simplified procedure for estimating a suitable T_2 is presented.

During the inelastic deformation of the system, period elongation is observed, which can be estimated via the secant stiffness, k_{eq}, obtained by

$$k_{eq} = k_e \frac{u_y}{u_m} \tag{11}$$

Rosenblueth and Herrera (1964) proposed a methodology for estimating the inelastic displacement of a system, using an equivalent linear system of period T_{eq}, stiffness k_{eq}, and damping ratio ζ_{eq}. The concept is that the energy dissipated by the original inelastic system of period T_1 and viscous damping ratio ζ_1, equals the energy dissipated by the equivalent linear system, within one cycle of oscillation in simple harmonic motion. For a system with bilinear force-displacement relationship, T_{eq} is obtained using the equation (e.g. Chopra and Goel 2001) below

$$T_{eq} = T_1 \sqrt{\frac{E(\mu_d)}{1 - \alpha + \alpha E(\mu_d)}} \tag{12}$$

where $E(\mu_d)$ is the mean μ_d at the R_y considered. An estimation of $E(\mu_d)$ can be obtained using the aforementioned relationships by Ruiz-Garcia and Miranda (2003).

Period T_{eq}, obtained using equation (12), is contrasted in Fig. 14 to the estimated period T_2 at which the maximum correlation coefficient was observed. It is observed that, the EDP points show a reasonable conformity to the T_{eq} curve. It is, therefore, concluded that the proposed procedure for calculating T_{eq} can be used to obtain a reasonable estimate of T_2.

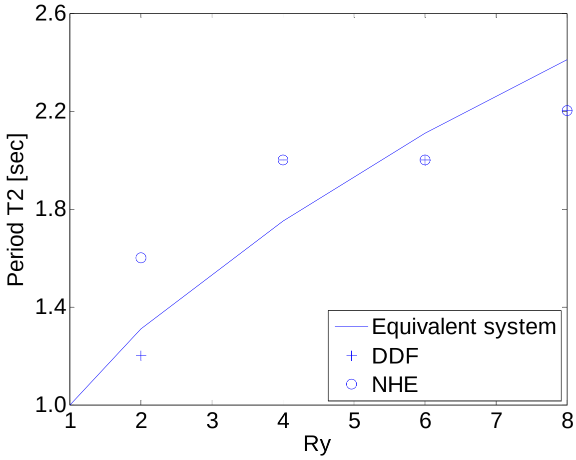

Fig. 14 Estimation of period T_2.

A significant factor affecting the optimum T_2 is the sequence of pulse intensities in the ground motion. The authors are not aware of any existing methodology that allows for the sequence of the ground motion pulse intensities. The present estimation of a suitable T_2 ignores this significant factor and approaches the problem from a statistical analysis perspective. The estimation error resulting from the number of 40 ground motions used was calculated previously, and it is acknowledged that a larger number would have resulted in a reduced error.

8.2 Practical calculation of $S_{dN}(T_1, T_2)$

The calculation of $S_{dN}(T_1, T_2)$ requires the prior calculation of $S_d(T)$ between T_1 and T_2. The spacing of the T intervals should be small enough, e.g. 0.01 sec, so as to capture the jaggedness of the response spectrum. In practical application, the $S_{dN}(T_1, T_2)$ of each record can be efficiently calculated using a computer program. Due to large number of T intervals, the manual calculation of $S_{dN}(T_1, T_2)$ is rather prohibitive.

9 Conclusions

A vector-valued IM has been presented, denoted as $\langle S_a(T_1), S_{dN}(T_1, T_2)\rangle$. The Normalized Spectral Area parameter, $S_{dN}(T_1, T_2)$, is evaluated by integration of the displacement response spectrum between periods T_1 and T_2, and normalization to $S_d(T_1)$. Due to the normalization, the $S_{dN}(T_1, T_2)$ value does not change when the ground motion is scaled. $S_{dN}(T_1, T_2)$ captures the effect of the ground motion frequency content and period elongation on the structural response. The proposed IM was developed with the intention of being used in a GMSM method aimed at estimating the damage state and collapse potential, wherein records are normalized to $S_a(T_1)$ and the estimation of the full distribution of the response is sought.

To evaluate the characteristics of the IM, dynamic analyses were conducted on a SDOF system using a dataset of 40 ground motion records. It was explained that by expressing ground motion intensity using R_y in the estimation of the response distribution, the problem of using unrealistic scale factors is avoided. The relative EDPs investigated were μ_d, and NHE. Regression analysis was then carried out between $\ln\left(S_{dN}(T_1, T_2)\right)$ and each of $\ln(\mu_d)$, and $\ln(NHE)$, using the simple linear model. The correlation coefficients at moderate to high nonlinearity levels were found to be in the range 0.6-0.8. The implication of such high correlation is that using the proposed IM with certain GMSM methods is expected to result in an optimized EDP prediction, contrasted to using an IM with lower correlation or to random selection. The parametric analysis carried out allows the generalization of the conclusions in the range of periods $T_1 = 0.5 - 2.0$ sec, and in the range of strain-hardening stiffness $a = 3\% - 10\%$. Regression analysis has confirmed that the upper integration period T_2, at which the peak ρ was observed, depends on the nonlinearity level. This finding can affect ground motion selection as applied in building codes.

Compared to $\langle S_a(T_1), \varepsilon \rangle$, the proposed IM was found to have generally higher correlation with the relative EDPs investigated. It was explained that the correlation between a relative IM, such as $S_{dN}(T_1, T_2)$, and a relative EDP, such as μ_d, is not dependent on the normalization of the ground motions, which means that the proposed IM can be used in both intensity-based assessments, and in scenario-based parametric studies. The use in scenario-based assessments of real systems has certain limitations. Finally, a procedure was proposed for estimating T_2, based on which a suitable $S_{dN}(T_1, T_2)$ can be found with respect to R_y.

10 Appendix

Table A1 presents the dataset of 40 records used in the dynamic analyses.

Earthquake	**Station**	**Mom. Magnitud**	**Epicentral**	**Azimuth /**	$S_a(T_1)$ **[m/sec^2**	$S_{dN}(1.0, 2.0$
Loma Prieta	CDMG 47379	6.93	28.64	000	1.088	1.60
18/10/1989 –	Gilroy Array #1			090	3.077	1.45
Victoria, Mexico	UNAMUCSD 6604	6.33	33.73	045	5.811	1.08
09/06/1980 –	Cerro Prieto			315	2.613	0.99
Coalinga	CDMG 46175	6.36	33.52	045	2.404	1.28
02/05/1983 –	Slack Canyon			315	2.652	1.18
San Fernando	CDMG 126	6.61	24.19	111	0.678	1.05
09/02/1971 –	Lake Hughes #4			201	1.096	0.95
Duzce, Turkey	Lamont 531	7.14	27.74	000	0.758	1.24
12/11/1999				090	1.580	1.14
Kozani, Greece	ITSAK 99999	6.40	18.27	L	1.245	1.10
13/05/1995 –	Kozani			T	0.652	0.79
Irpinia, Italy	ENEL 99999	6.20	22.29	000	0.604	0.98
23/11/1980 –	Bagnoli Irpinio			270	0.638	1.19
Whittier Narrows	CDMG 24399	5.99	19.56	000	0.475	0.89
01/10/1987 –	Mt Wilson - CIT			090	0.259	0.67
Basso Tirreno	Milazzo	6.00	34	NS	0.396	0.94
15/04/1978 –				EW	0.312	1.26
Montenegro	Hercegnovi Novi –	6.90	65	NS	1.684	0.80
15/04/1979 –	Pavicic School			EW	1.680	0.99
Tabas, Iran	9102 Dayhook	7.35	20.63	LN	2.200	1.36
16/09/1978				TR	3.376	1.29
Umbria Marche	Assisi-Stallone	6.00	21	NS	0.468	1.18
26/09/1997				EW	0.231	1.77
North Palm	CDMG 12206 Silent	6.06	20.70	000	0.174	1.05
Springs	Valley - Poppet Flat			090	0.362	0.69

Loma Prieta	USGS 1032	6.93	49.52	270	0.864	0.91
18/10/1989 –	Hollister –			360	0.962	0.82
Chi-Chi, Taiwan	CWB 99999	7.62	77.50	N	4.248	1.06
20/09/1999	TCU045			E	2.922	1.09
Northridge	USC 90059 Burbank	6.69	23.18	060	0.879	1.16
17/01/1994 –	–			330	0.891	1.16
San Fernando	USGS 266 Pasadena	6.61	39.17	180	0.623	1.09
09/02/1971 –	–			270	1.388	0.83
Whittier Narrows	USC 90017	5.99	28.48	075	0.126	1.30
01/10/1987 –	LA - Wonderland			165	0.103	1.02
Northridge	USGS 5080 Monte	6.69	19.19	270	0.492	1.01
17/01/1994 –	Nido Fire Station			360	1.118	0.95
Irpinia, Italy	Auletta	6.90	33.10	000	0.469	1.83
23/11/1980 –				270	0.651	1.67

Table A1. Ground motion records.

References

Ambraseys N, Smit P, Sigbjornsson R, Suhadolc P, Margaris, B. (2002) Internet-Site for European Strong-Motion Data, European Commission, Research-Directorate General, Environment and Climate Programme. http://smbase.itsak.gr/. Accessed 19 September 2012.

Ay BÖ, Akkar S. (2012) A procedure on ground motion selection and scaling for nonlinear response of simple structural systems, Earthquake Engineering and Structural Dynamics; 41(12): 1693-1707. DOI: 10.1002/eqe.1198.

Baker JW, Cornell CA. (2006) A vector-valued ground motion intensity measures for probabilistic seismic demand analysis, Report 2006/08. Pacific Earthquake Engineering Center, Stanford University, California.

Bojórquez E, Iervolino I. (2011) Spectral shape proxies and nonlinear structural response. Soil Dynamics and Earthquake Engineering; 31 (7): 996-1008. DOI: 10.1016/j.soildyn.2011.03.006.

Bojórquez E, Iervolino I, Reyes-Salazar A, Ruiz SE. (2012) Comparing vector-valued intensity measures for fragility analysis of steel frames in the case of narrow-band ground motions. Engineering Structures; 45: 472-480. DOI: 10.1016/j.engstruct.2012.07.002.

Bradley BA. (2011) Empirical equations for the prediction of displacement spectrum intensity and its correlation with other intensity measures. Soil Dynamics and Earthquake Engineering; 31 (8): 1182-1191. DOI: 10.1016/j.soildyn.2011.04.007.

Buratti N, Stafford PJ, Bommer JJ. (2011) Earthquake accelerogram selection and scaling procedures for estimating the distribution of drift response. Journal of Structural Engineering, American Society of Civil Engineers; 137 (3): 345-357. DOI: 10.1061/(ASCE)ST.1943-541X.0000217.

Chopra AK, Goel RK. (2001) Direct displacement-based design: Use of inelastic vs elastic design spectra. Earthquake Spectra; 17 (1): 47-64. DOI: 10.1193/1.1586166.

Clough RW, Johnston SB. (1966) Effect of stiffness degradation on earthquake ductility requirements. Proceedings of the Japan Earthquake Engineering Symposium.

Conte JP, Pandit H, Stewart JP, Wallace JW. (2003) Ground motion intensity measures for performance-based earthquake engineering, Proceedings of the 9th International Conference in Applied Statistics and Probability in Civil Engineering, San Francisco, USA.

Cordova PP, Dierlein GG, Mehanny SSF, Cornell CA. (2001) Development of a two parameter seismic intensity measure and probabilistic assessment procedure. Proceedings of the second US-Japan workshop on performance-based earthquake engineering methodology for reinforced concrete building structures, Japan pp 195-212.

Cornell CA, Krawinkler H. (2000) Progress and challenges in seismic performance assessment. PEER Center News 3 (2).

Fajfar P, Vidic T, Fischinger M. (1990) A measure of earthquake motion capacity to damage medium-period structures. Soil Dynamics and Earthquake Engineering 9 (5): 236–242.

Haselton CB. (2009) Evaluation of ground motion selection and modification methods, PEER Report 2009/01. Pacific Earthquake Engineering Centre, University of California, Berkeley.

Housner GW. (1952) Intensity of ground motion during strong earthquakes. Earthquake Research Laboratory, California Institute of Technology, Pasadena, California.

Hutchinson TC, Chai YH, Boulanger RW, Idriss IM. (2002) Inelastic seismic response of extended pile shaft supported bridge structures, Report 2002/14. Pacific Earthquake Engineering Center, Stanford University, California.

Iervolino I, Cornell CA. (2005) Record selection for nonlinear seismic analysis of structures. Earthquake Spectra 21 (3): 685-713. DOI: 10.1193/1.1990199.

International Conference of Building Officials (1997) Uniform Building Code, Volume 2: structural engineering design provisions. Whittier, California.

Jacobsen LS. (1930) Steady forced vibrations as influenced by damping. ASME Transactions 52 (1): 169-181.

Lilliefors HW. (1967) On the Kolmogorov-Smirnov test for normality with mean and variance unknown. Journal of the American Statistical Association 62 (318): 399–402.

Mahin SA, Bertero VV. (1981) An evaluation of seismic design spectra. Journal of Structural Division, Proceedings of ASCE 107 (ST9): 1777-1795.

Mahin SA, Lin J. (1983) Construction of inelastic response spectra for single degree of freedom systems. UCB/EER-83/17, Earthquake Engineering Research Center, University of California at Berkley.

Pacific Earthquake Engineering Research Center. (2005) NGA Database 2005. University of California at Berkley. http://peer.berkeley.edu/nga/. Accessed 18 February 2015.

Park YJ, Ang AH-S. (1985) Mechanistic seismic damage model for reinforced concrete. Journal of Structural Engineering, American Society of Civil Engineers 111 (4): 722–739. DOI: 10.1061/(ASCE)0733-9445(1985)111:4(722).

Park YJ, Ang AH-S, Wen YK. (1985) Seismic damage analysis of reinforced concrete buildings. Journal of Structural Engineering, American Society of Civil Engineers 111 (4): 740–757. DOI: 10.1061/(ASCE)0733-9445(1985)111:4(740).

Rosenblueth E, Herrera I. (1964) On a kind of hysteretic damping. Journal of the Engineering Mechanics Division, Proceedings of the American Society of Civil Engineers 90 (EM4): 37-48.

Ruiz-Garcia J, Miranda E. (2003) Inelastic displacement ratios for evaluation of existing structures. Earthquake Engineering and Structural Dynamics 32 (8): 1237-1258. DOI: 10.1002/eqe.271.

Ruiz-Garcia J, Miranda E. (2006) Residual displacement ratios for assessment of existing structures. Earthquake Engineering and Structural Dynamics 35 (3): 315-336. DOI: 10.1002/eqe.523.

Sachs L. (1984) Applied Statistics – A Handbook of Techniques, second edition. Springer-Verlag.

Shome N, Cornell CA, Bazzuro P, Carballo JE. (1998) Earthquakes, records and nonlinear responses. Earthquake Spectra 14 (3): 469-500. DOI: 10.1193/1.1586011.

Theophilou AI. (2013) A ground motion selection and modification method suitable for probabilistic seismic assessment of building structures, PhD Thesis. Faculty of Engineering and Physical Sciences, University of Surrey, Surrey, UK.

Theophilou AI, Chryssanthopoulos MK. (2011) A ground motion record selection procedure utilizing a vector-valued IM incorporating normalized spectral area. Proceedings of the 11th International Conference of Applied Statistics and Probability in Civil Engineering, Zurich, Switzerland.

Trifunac MD, Brady AG. (1975) A study on the duration of earthquake strong motion. Bulletin of the Seismological Society of America 65 (3): 581–626.

Van Soest J. (1967) Some experimental results concerning tests of normality. Statistica, Neerlandica 21: 91–97.

Von Thun JL, Roehm LH, Scott GA, Wilson JA. (1988) Earthquake ground motions for design and analysis of dams. Earthquake Engineering and Soil Dynamics II—Recent Advances in Ground-Motion Evaluation, Geotechnical Special Publication, American Society of Civil Engineers 20:463–481.